Eur. Phys. J. A **31**, 649–652 (2007)
DOI 10.1140/epja/i2006-10209-3

THE EUROPEAN PHYSICAL JOURNAL A

Special Article – QNP 2006

X(1859) Baryonium or something else?

D.R. Entem[a] and F. Fernández

Nuclear Physics Group and IUFFyM, University of Salamanca, E-37008 Salamanca, Spain

Received: 25 October 2006
Published online: 26 February 2007 –

Abstract. Using a constituent-quark model we study possible bound or resonance $N\bar{N}$ states. The model fits the $p\bar{p}$ and $p\bar{n}$ cross-sections and explains the large $^3P_0$ antiprotonium energy shift. Only a resonance is found in the $^3P_0$ $I = 0$ partial wave. The threshold enhancement in the $J/\Psi \to \gamma p\bar{p}$ decay can be explained with FSI effects in S-waves and no $N\bar{N}$ bound state is needed.

PACS. 12.39.Jh Non relativistic quark model – 13.75.Cs Nucleon-nucleon interactions (including antinucleons, deuterons, etc.) – 25.43.+t Antiproton-induced reactions – 21.10.Dr Binding energies and masses

1 Introduction

The recent observation of a near threshold narrow enhancement in the $p\bar{p}$ invariant-mass spectrum from radiative $J/\psi \to \gamma p\bar{p}$ decay by the BES Collaboration [1] has renewed the interest for the $N\bar{N}$ interaction and its possible baryonium bound states. If this enhancement is fitted with an S-wave Breit-Wigner resonance function the resulting peak mass is $M = 1859 \pm 6\,\mathrm{MeV}$, which is below the $p\bar{p}$ threshold, whereas a P-wave fit gives a peak mass very close to the threshold at $M = 1876 \pm 0.9\,\mathrm{MeV}$. The photon polar angle distribution is consistent with $1+\cos^2\theta$ which suggest that the total angular momentum is very likely to be $J = 0$. So this structure may have quantum numbers $J^{PC} = 0^{-+}$ or $J^{PC} = 0^{++}$ which, in principle, do not correspond to any known meson resonance. However, no similar signal was observed by BES in the $\pi^0 p\bar{p}$ channel which suggests that the enhancement is due to an isoscalar resonance.

The simplest interpretation of the experimental $J/\psi \to \gamma p\bar{p}$ is a baryonium bound state [2,3] although the result is currently being interpreted in several ways [4–6].

The study of the possible nucleon-antinucleon bound states has a very long history (see ref. [7] and references therein). Usually the real part of the $N\bar{N}$ interaction is derived by G-parity transformation of the NN potentials [7]. The derivation of the annihilation part is still a major challenge. Although some complicate microscopic models have been developed the best results are obtained by phenomenological treatments.

In the meson exchange picture the central force in the NN sector is provided basically by the σ and the ω which have opposite signs but adds in $N\bar{N}$. This gives a lot of attraction and usually generates many $N\bar{N}$ bound states. The ω-exchange contribution is replaced in quark based models by the antisymmetry which is not present in $N\bar{N}$. Therefore quark-based $N\bar{N}$ potentials may look different from the conventional ones. Furthermore, the NN one-pion exchange tensor interaction is attenuated also by antisymetrization and not by ρ-exchanges. This fact, which has observable consequences at the NN level [8], may also significantly change the whole $N\bar{N}$ interaction.

2 The N$\bar{\text{N}}$ interaction

We use the constituent-quark model from refs. [9,10] as the microscopic model to get the $N\bar{N}$ interaction. The model takes into account spontaneous chiral symmetry-breaking through pseudo-goldstone boson modes and the constituent mass generation. Perturbative QCD corrections beyond the chiral symmetry-breaking scale are included through fluctuations of the one-gluon field which give gluon exchange diagrams.

In the $N\bar{N}$ system, it is not allowed any quark-antiquark exchange between N and $\bar{N}$. However quark-antiquark annihilation has to be considered. This makes important differences with the NN system in which exchange diagrams are important. For example the one-gluon exchange only contributes in the $N\bar{N}$ case through annihilation diagrams which are not present in the NN sector.

In order to get the $q\bar{q}$ interaction, we have to perform a G-parity transformation of the qq potentials. For the pseudo-scalar case only a -1 factor is needed while the scalar case remains unchanged. For the real part of the annihilation diagrams we use the derivation from [11].

[a] e-mail: entem@usal.es

Once the microscopic model is fixed we use the Resonating Group Method to derive the $N\bar{N}$ interaction in the same way as we did in the NN case. The N and $\bar{N}$ wave functions are the same provided that we use for the spin-isospin of the $\bar{N}$ the G-parity transformed.

In order to have a realistic model it is important to include the annihilation into mesons. Annihilation processes are very complicated, for a review see [12]. There are microscopic models at quark level that describes such processes. Usually these models are highly non-local and energy dependent, and instead of using one of these, we chose to describe such processes with an optical potential in order to simplify the calculation. This approximation was already used by Bryan and Phillips [13], Dover and Richard [14] and Kohno and Weise [15]. We chose the parametrization

$$V_{q\bar{q}}^{Anh}(\boldsymbol{q}) = i\, W_i\; e^{-\frac{q^2 b'^2}{3}}, \tag{1}$$

where W_i gives the strength and b' the range. All but these two parameters of the model are fixed by the NN sector and we use those of [9]. b' and W_i are fixed fitting the total annihilation cross-section for the $p\bar{p}$ system, since the imaginary part of the potential dominates it. We use the values $W_i = -0.74\,\mathrm{GeV}^{-2}$ and $b' = 0.848\,\mathrm{fm}$. With these two parameters we are able to fit the annihilation data in the laboratory momentum range between 100 and 600 MeV as shown in fig. 1(a).

3 Results

Once the annihilation cross-section is fitted, we calculate the total cross-section, which comes in good agreement with the experimental data as can be seen in fig. 1(b). This indicates that the real part of the interaction should be fairly well.

We check the isospin dependence studying the $p\bar{n}$ reaction. Notice that we do not include any isospin dependence in the annihilation potential, so all the isospin dependence comes from the real part of the potential and is fixed from the NN sector. As can be seen in figs. 2 (a) and (b) the results, given by the solid line, are in agreement with the data for the total and annihilation cross-sections, although in both cases there are big uncertainties.

Now we are in the position to study possible $N\bar{N}$ bound states. If we do not include the imaginary potential, the real part of the potential predicts two bound states. One has quantum numbers $J^{PC} = 1^{--}$ which is a $^3S_1$-$^3D_1$ partial wave in $I = 0$ and the other is $J^{PC} = 0^{++}$ which is a $^3P_0$ state also with $I = 0$. Both states are very close to threshold being the binding energy 1.30 MeV for the first one and 1.32 MeV for the second one. We find the strongest interactions in S-waves with $I = 0$ which is much bigger than $I = 1$ and for the $^3P_0$ wave for $I = 0$ which is also much bigger than for $I = 1$.

When we include the annihilation potential the 1^{--} state is washed out and the 0^{++} state is transformed in a near-threshold resonance with a mass 18.5 MeV above threshold and a width of 33.6 MeV.

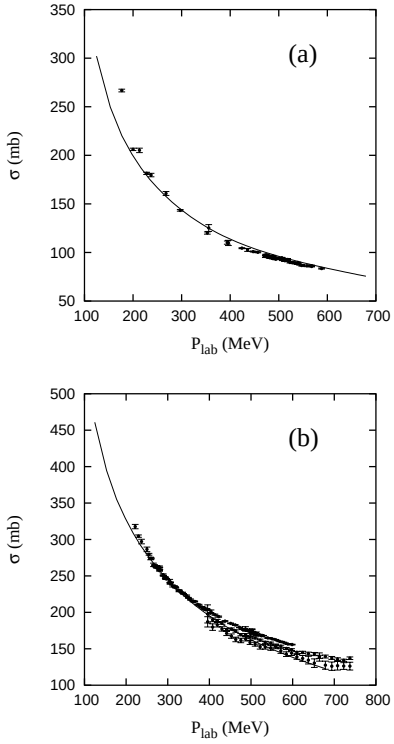

Fig. 1. $p\bar{p}$ annihilation (a) and total (b) cross-sections. Experimental data are from ref. [16].

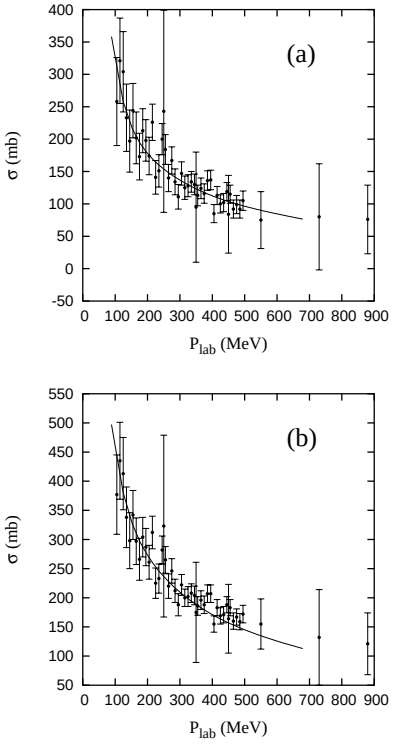

Fig. 2. $p\bar{n}$ annihilation (a) and total (b) cross-sections. Experimental data are from ref. [17].

Table 1. $p\bar{p}$ energy shifts calculated from the improved Trueman formula (ΔE) and from perturbation theory including only $p\bar{p}$ states ($\Delta E_{p\bar{p}}$) and the coupling to $n\bar{n}$ ($\Delta E_f = \Delta E_{p\bar{p}} + \Delta E_{n\bar{n}}$). S-waves are in eV while P-waves are in meV. Experimental values are available on partial waves $\Delta E_{exp}(1\,^1S_0) = 440 \pm 75 - i(600 \pm 125)$ eV [18] and $\Delta E_{exp}(2\,^3P_0) = -140 \pm 28 - i(60 \pm 12)$ meV [19].

State	ΔE	$\Delta E_{p\bar{p}}$	ΔE_f
$1\,^1S_0$	$557.3 - i820.9$	$-587.5 - i2263.4$	
$2\,^1S_0$	$67.7 - i106.3$	$-73.4 - i28.3$	
$2\,^1P_1$	$-27.9 - i12.4$	$-27.0 - i10.4$	$-28.5 - i10.4$
$2\,^3P_0$	$-67.3 - i94.7$	$-71.8 - i10.4$	$-112.2 - i26.0$
$2\,^3P_1$	$36.5 - i10.9$	$40.1 - i10.4$	$29.6 - 12.1$

This resonance may explain the data from antiprotonic atoms which indeed are the only low energy data available. The protonium atomic levels are shifted and widened $\Delta E_{nl} = \delta E_{nl} - i\Gamma_{nl}/2$ by the strong interaction. One of the most interesting outcomings is that the $^3P_0$ protonium level shift is much bigger than any other. This result suggests the existence of a near threshold $N\bar{N}$ resonance which enhances the scattering amplitude. The energy shifts in hadronic atoms can be determined with the improved Trueman formula [20,7], using the scattering length (S-wave) or the scattering volume (P-waves):

$$\delta E_{nl} = -E_n \frac{4}{n} \frac{a_l}{a_B^{2l+1}} \alpha_{nl} \left(1 - \frac{a_l}{a_B^{2l+1}} \beta_{nl} + \ldots\right). \qquad (2)$$

An alternative approach is to use perturbation theory that for weak potentials reproduce the former result. However, the strong interaction in S-waves is big enough compared to the coulombic at short range that perturbation theory does not work. For P-waves the centrifugal barrier contributes to soften the strong interaction, and perturbation theory became useful.

We use the improved Trueman formula to calculate the energy shifts and half-width for the $p\bar{p}$ $L = 0$ and $L = 1$ partial waves. The results are shown in table 1. We also include the results of the perturbative calculation for the P-waves, which are compatibles with the one calculated with the Trueman formula. One can see from this table that the experimental results are well reproduced except for the $^3P_0$ energy shift which is underestimate by a factor two. These predictions coincide basically with those obtained with other potentials [21].

It is worth to note that $p\bar{p}$ and $n\bar{n}$ channels are coupled and it may have a significant influence in the theoretical predictions. So for P-waves we use coupled channel perturbation theory. Results are shown in table 1. As we can see the coupling with the $n\bar{n}$ channel does not affect very much to the energy shift except for the $^3P_0$ partial wave. The observed enhancement in this wave is due to the resonance located close to the $N\bar{N}$ threshold in this channel.

As we do not find any bound state we have studied FSI effects in the $J/\Psi \to \gamma p\bar{p}$ as a possible justification of the threshold enhancement. Using the Watson-Migdal prescription we find that it can be explained with FSI in S-waves. The result for the $^1S_0$ partial wave are shown in fig. 3. A more elaborate analysis is on preparation.

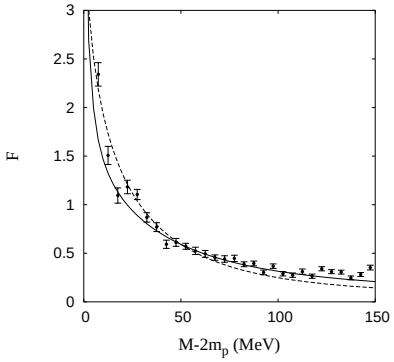

Fig. 3. $J/\Psi \to \gamma p\bar{p}$ invariant-mass distribution. Lines show the FSI factor for the $^1S_0$ $I = 0$ (solid) and $I = 1$ (dashed) channels. Experimental data are from [1,6].

This work has been partially funded by MEC under Contract No. FPA2004-05616, and by Junta de Castilla y León under Contract No. SA-104/04.

References

1. BES Collaboration (J.Z. Bai *et al.*), Phys. Rev. Lett. **91**, 022001 (2003).
2. A. Datta, P.J. O'Donnell, Phys. Lett. B **567**, 273 (2003).
3. B. Loiseau, S. Wycech, Phys. Rev. C **72**, 011001(R) (2001).
4. Tao Huang, Shi-Lin Zhu, Phys. Rev. D **73**, 014023 (2006).
5. Bing An Li, Phys. Rev. D **74**, 034019 (2006).
6. A. Sibirtsev, J. Haidenbauer, S. Krewald, Ulf-G. Meissner, A.W. Thomas, Phys. Rev. D **71**, 054010 (2005).
7. E. Klempt, F. Bradamante, A. Martin, J.-M. Richard, Phys. Rep. **368**, 119 (2002).
8. F. Fernández, A. Valcarce, P. González, V. Vento, Phys. Lett. B **287**, 35 (1992).
9. D.R. Entem, F. Fernández, A. Valcarce, Phys. Rev. C **62**, 034002 (2000).
10. A. Valcarce, H. Garcilazo, F. Fernández, P. González, Rep. Prog. Phys. **68**, 965 (2005); J. Vijande, F. Fernández, A. Valcarce, J. Phys. G **19**, 2013 (2005).
11. A. Faessler, G. Lübeck, K. Shimizu, Phys. Rev. D **26**, 3280 (1982).
12. E. Klempt, C. Batty, J.-M. Richard, Phys. Rep. **413**, 197 (2005).
13. R.A. Bryan, R.J. Phillips, Nucl. Phys. B **5**, 201 (1986); **7**, 481 (1986) (E).
14. C.B. Dover, J.-M. Richard, Phys. Rev. C **21**, 1466 (1980); J.-M. Richard, M.E. Saino, Phys. Lett. B **110**, 349 (1982).
15. M. Kohno, W. Weise, Nucl. Phys. A **454**, 429 (1986).
16. W. Brückner *et al.*, Z. Phys. A **335**, 217 (1990); T. Kamae *et al.*, Phys. Rev. Lett. **44**, 1439 (1980); K. Nakamura *et al.*, Phys. Rev. D **29**, 349 (1984); A.S. Clough *et al.*, Phys. Lett. B **146**, 299 (1984); D.V. Bugg *et al.*, Phys. Lett. B **194**, 563 (1987).

17. B. Gunderson, J. Learned, J. Mapp, D.D. Reeder, Phys. Rev. D **23**, 587 (1981); T. Armstrong *et al.*, Phys. Rev. D **36**, 659 (1987).
18. M. Augsburger *et al.*, Nucl. Phys. A **658**, 149 (1999).
19. D. Gotta *et al.*, Nucl. Phys. A **660**, 283 (1999).
20. T.L. Trueman, Nucl. Phys. **26**, 57 (1961).
21. J. Carbonell, M. Mangin-Brinet, Nucl. Phys. A **692**, 11c (2001).